IJPSR (2022), Volume 13, Issue 2 **(Research Article)**

INTERNATIONAL JOURNAL OF PHARMACEUTICAL SCIENCES AND RESEARCH

Received on 16 May 2021; received in revised form, 10 June 2021; accepted, 21 June 2021; published 01 February 2022

FORMULATION AND CHARACTERIZATION OF IBRUTINIB LOADED CYCLODEXTRIN NANOSPONGES

G. Surendar * and B. Ramesh

Department of Pharmacy, Career Point University, Kota - 325003, Rajasthan, India.

Keywords:

Ibrutinib, Bruton's tyrosine kinase,β - Cyclodextrin, Nanosponges, Taguchi method.

Correspondence to Author:
Mr. G. Surendar

Research Scholar,
Department of Pharmacy,
Career Point University, Kota - 325003, Rajasthan, India.

E-mail: dbpathi71@gmail.com

ABSTRACT: The aim of this study was to explore the feasibility of complexing the poorly water-soluble drug ibrutinib with β-cyclodextrin (β-CD) based nanosponges (NS), which offer advantages of improving dissolution rate and eventually oral bioavailability. Blank NS were fabricated by reacting β-CD with the cross-linker carbonyldiimidazole at different molar ratios (1:2, 1:4 and 1:8). The effect of formulation parameters on practical yield and particle size were evaluated by L9 Taguchi orthogonal array design. The NS of highest solubilization extent for the drug were complexed with ibrutinib. Drug-loaded NS (IBNS) were characterized for various physicochemical properties. The optimized IBNS showed a particle size of 138 nm during a zeta potential of -21.6 mV. The drug loading capacity was 48%. More than 90% of the drug was released from IBNS2 over 24 h while that of free drug suspension was only 21%. The DSC, FT-IR, and PXRD studies confirmed the complexation of ibrutinib with NS and the amorphous state of the drug in the complex. Hence, the solubility and dissolution of the nanosponge formulation were significantly enhanced compared with the plain ibrutinib.

INTRODUCTION: β-Cyclodextrin - based nanosponges play an important role in new arrays of agriculture, floriculture, cosmetics, medicine, high molecular weight proteins, novel flame retardants, gas carriers, and water filters. In recent years, the field of advance nanostructured systems witnesses rapid development due to miniaturization, dose-reduction, sustained and controlled. Release of actives and long-term stability of the material.

QUICK RESPONSE CODE

DOI: 10.13040/IJPSR.0975-8232.13(2).930-41

This article can be accessed online on www.ijpsr.com

DOI link: http://dx.doi.org/10.13040/IJPSR.0975-8232.13(2).930-41

β-CDNSs are colloidal and cross-linked nanocarriers comprising solid mesh-like structures with nano-cavities for encapsulation of complex lipophilic and hydrophilic chemical substances [1]. The release of enthalpy-rich water molecules from the polymeric structures accounts for high complexation efficiency with different molecular substrates.

The advantages of β-CDNS involve the sustained and controlled release of entrapped molecules with high efficiency and excellent stability. Thus, nanosponges are an effective carrier for delivering actives and developed as a commercial drug delivery system in pharmaceutical industries after certified clinical studies. In the near future, the β-CDNS-based product will capture the market due to its diverse applications in anti-cancer, antiviral,

antiplatelet, antihypertensive therapy, *etc.* [2] Ibrutinib is a selective and covalent inhibitor of the enzyme Bruton's tyrosine kinase (BTK), it is used for the treatment of B-cell malignancies [3]. Apart from the BTK, ibrutinib has been heavily reported to efficiently block the activation of several other kinases such as ITK, TEC, TFK, JAK [3], HCK, BLK and especially ERBB receptor family, indicating that ibrutinib can be exploited for the treatment of multiple tumors in the future [4].It has been reported to exhibit pH-dependent solubility as it is slightly soluble at pH 1.2 while practically insoluble at pH 3 to 8, which leads to low bioavailability and impedes its *in-vivo* antitumor effect after oral administration [5]. Taguchi developed a method for designing experiments to investigate how different parameters affect the mean and variance of a process performance characteristic that defines how well the process is functioning. The experimental design proposed by Taguchi involves using orthogonal arrays to organize the parameters affecting the process and the levels at which they should be varied. Instead of having to test all possible combinations like the factorial design, the Taguchi method tests pairs of combinations. This allows for collecting the necessary data to determine which factors most affect product quality with a minimum amount of experimentation, thus saving time and resources. The Taguchi method is best used when there is an intermediate number of variables (3 to 50), few interactions between variables, and when only a few variables contribute significantly [6]. The current research deals with the formulation and evaluation of ibrutinib loaded β-Cyclodextrin nanosponges for prolonged drug release and enhanced bioavailability.

MATERIALS AND METHODS:

Materials: B-Cyclodextrin (Complexol-B) was obtained as a gift sample from Gangwal Chemicals Pvt. Ltd. (Mumbai, India). Carbonyldiimidazole was purchased from Sigma Aldrich (Milan, Italy). Ibrutinib was obtained as a gift sample from MSN laboratories Pvt. Ltd. Hyderabad, India. All other chemicals and reagents used in the study were of analytical grade. Milli Q water (Millipore) was used throughout the studies.

Preparation of β-cyclodextrin Nanosponges: Cyclodextrin-based nanosponges were prepared using carbonyldiimidazole for the cross-linking as reported elsewhere [7]. Three types of nanosponges (NS1-NS3) were prepared using different molar ratios of reactants **Table 1.** by dissolving anhydrous β-Cyclodextrinin dimethyl sulphoxide followed by addition of carbonyldiimidazole and refluxed in an oil bath.

TABLE 1: MOLAR RATIOS AND CONCENTRATIONS OF CYCLODEXTRINS AND THE CROSS-LINKER

S. no.	Type of NS	Molar ratio	Concentration of β-cyclodextrin (gms)	Concentration of carbonyldiimidazole (gms)
1	NS1	1:2 (β-CD:CDI)	2.274	2.484
2	NS2	1:4 (β-CD:CDI)	2.274	4.968
3	NS3	1:8 (β-CD:CDI)	2.274	9.936

TABLE 2: VARIABLES, FACTORS AND THEIR LEVELS USED IN L9 TAGUCHI ORTHOGONAL ARRAY DESIGN

Independent variables			Levels		
Variable	Name	Units	-1	0	+1
A	Reaction temperature	°C	80	100	120
B	Reaction time	min	360	420	480
C	Stirring speed	rpm	1000	2000	3000
D	Volume of solvent	ml	100	150	200
Dependent variable			**Goal**		
Y1	Practical yield	%	Maximize		
Y2	Particle size	nm	Minimize		

Optimization of Reaction Conditions [8]: The optimization of nanosponges was carried out by Taguchi orthogonal array design for investigating the effects of major factors on responses. Stat-Ease Design Expert® software V8.0.1 was used for the optimization wherein the reaction temperature (A), reaction time (B), stirring speed (C), and volume of solvent (D) were varied so as to identify their optimum conditions for the synthesis of nanosponges with reduced particle size, maximum

practical yield **Table 2.** The statistical analysis of the results using analysis of variance was performed to determine the factors which had a paramount influence on particle size and practical yield.

Characterization of Nanosponges [9]:

Particle Size, Polydispersity Index and Zeta Potential: The particle size distribution and zeta potential were analyzed using a Mastersizer 2000 (Malvern Instruments Ltd, Worcestershire, UK).

Fourier Transformed Infrared (FTIR) Spectroscopy, X-Ray Powder Diffraction (XRPD) and Differential Scanning Calorimetry (DSC), Transmission Electron Microscopy (TEM): The FTIR spectra recorded by KBr disc method using Tensor 27 FTIR Spectrophotometer (Bruker Optics, Germany) in the region of 4000 to 600 cm^{-1}. X-ray powder diffraction patterns were recorded on an X-ray diffractometer (Bruker D8 Advance) at a scan rate of 5 °C / min in the 2θ range from 2.5 °C to 60 °C. DSC analysis carried out using a Perkin Elmer DSC/7 differential scanning calorimeter (Perkin-Elmer, CT-USA). The morphology of the nanosponges was observed under transmission electron microscopy (JEM-2000 EXII; JEOL, Tokyo, Japan).

Preparation of Ibrutinib-Loaded B-Cyclodextrin Nanosponges (IBNS): Ibrutinib loaded nanosponges (IBNS1, IBNS2, and IBNS3) were prepared by lyophilization technique as reported elsewhere 10 by suspending 200 mg of nanosponges in 100 ml of Milli Q water followed by addition of 100 mg of the drug. The colloidal supernatant was separated and freeze-dried using a lyophilizer (LARK INDIA) at a temperature of -20 °C and pressure of 13.33 mbar.

Physico-chemical Characterization of IBNS: Particle size, polydispersity index, and zeta potential were determined as per the procedure adopted for β-Cyclodextrinna nosponges. The formulations were analysed for FTIR, DSC, PXRD, TEM as per the procedure adopted for analysis of β-Cyclodextrin nanosponges.

Determination of Ibrutinib loading in IBNS11: Weighed quantity of IBNS was dissolved in methanol and then analyzed on a UV spectrophotometer (Labindia UV-3000 + UV-Vis Spectrophotometer) at 260 nm. The percent drug loading was calculated using the following formula

% Drug loading = Weight of drug-loaded in/ Initial weight of the drug

In-vitro Release of IBNS: *In-vitro* dissolution study of NS formulations and free ibrutinib was performed using multi-compartment (n=6) rotating cells with a dialysis membrane (Sartorius cut off 12,000 Da). The membrane was activated as per the procedure provided by the manufacturer. Formulation equivalent to 5 mg of ibrutinib was filled in the dialysis bag and placed in donor phase consists of 100 ml simulated gastric fluid (pH 6.4). The receptor phase also contains the same medium. The receptor phase was added with 0.5% w/v sodium lauryl sulphate (1 ml) to maintain proper sink conditions. The receptor phase was completely withdrawn at specified intervals and evaluated (Labindia UV-3000+ UV-Vis Spectrophotometer) at 260 nm [12].

Kinetic Analysis [13]: To elucidate the mode and mechanism of drug release, the data from the *in-vitro* release study were fitted into various kinetic models.

TABLE 3: TAGUCHI ORTHOGONAL ARRAY DESIGN WITH OBSERVED RESPONSES

Run	Reaction temperature (°C)	Reaction time (min)	Stirring speed (rpm)	Volume of solvent (ml)	Practical yield (%)	Particle size (nm)
1	80	480	3000	200	68.1	189
2	120	360	3000	150	83.5	169
3	100	480	1000	150	96.9	352
4	100	420	3000	100	94.6	142
5	80	360	1000	100	63.3	316
6	120	480	2000	100	88.2	213
7	100	360	2000	200	91.2	272
8	80	420	2000	150	66.2	242
9	120	420	1000	200	86.4	390

RESULTS AND DISCUSSION: Through preliminary screening reaction temperature, reaction time, stirring speed and volume of solvent were identified as the most significant process variables for the synthesis of nanosponges. In this study, a four-variable, three -level values matrix was constructed with the target output parameter being the practical yield and particle size. The Taguchi array, which led to an optimized combination through experiments **Table 3** [9].

Design Summary

Study Type	Factorial	Runs	9
Design Type	Taguchi OA	Blocks	No Blocks
Center Points	0		
Design Model	Main effects	Build Time (ms)	94.02

Factor	Name	Units	Type	Subtype	Low Actu	High Actual		
A	Reaction temperature	°C	Categoric	Nominal	80	120	Levels:	3
B	Reaction time	mn	Categoric	Nominal	360	480	Levels:	3
C	Stirring speed	rpm	Categoric	Nominal	1000	3000	Levels:	3
D	Volume of solvent	ml	Categoric	Nominal	100	200	Levels:	3

Response	Name	Units	Obs	Analysis	Minimum	Maximum	Mean	Std. Dev.	Ratio	Trans	Model
Y1	Practical yield	%	9	Factorial	63.3	96.9	82.0444	12.8354	1.53081	None	RMain effects
Y2	Particle size	nm	9	Factorial	142	390	253.889	85.2107	2.74648	None	RMain effects

FIG. 1: SUMMARY OF THE SELECTED TAGUCHI OA DESIGN

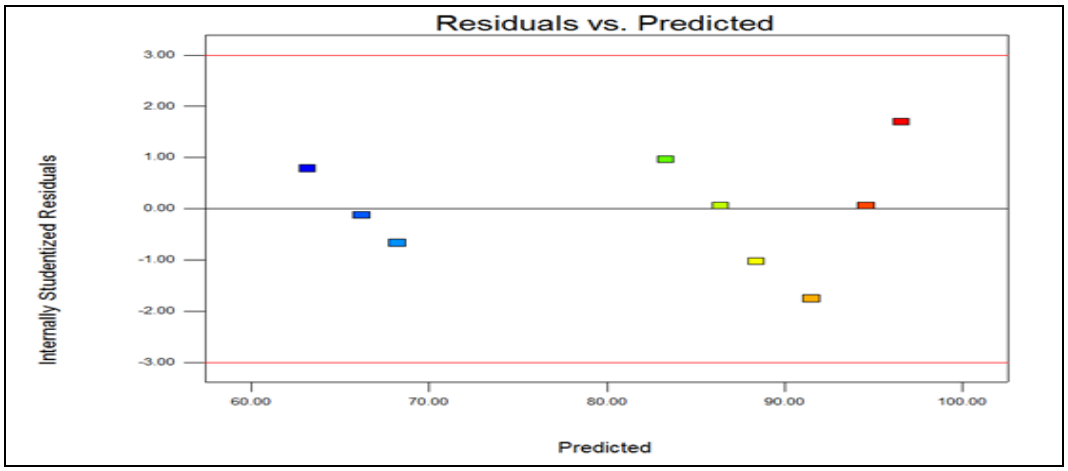

FIG. 2A: STUDENTIZED RESIDUALS VERSUS PREDICTED RESPONSE (PRACTICAL YIELD) BY THE FINAL MODEL

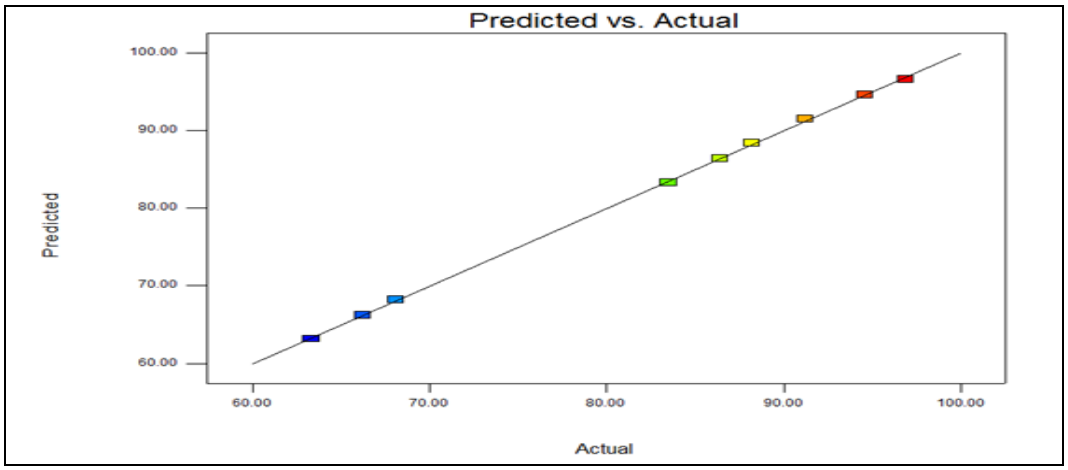

FIG. 2B: PREDICTED VERSUS ACTUAL VALUES OF PRACTICAL YIELD BY THE FINAL MODE

Effect of Process Parameters on Practical Yield: **Table 4.** shows the main effects of the various factors on the practical yield of nanosponges. The Model F-value of 4328.14 implies the model is significant. ANOVA has shown that the process parameters have a significant effect (Prob. F < 0.0001) on practical yield. **Fig. 2** indicates excellent agreement between the model and experimental data.

Effect of Process Parameters on Particle Size: **Table 4**. shows the main effects of the various factors on the particle size of nanosponges. The Model F-value of 302.943 implies the model is significant. ANOVA has shown that the process parameters significantly affect particle size (Prob. F < 0.0001). **Fig. 3.** indicates excellent agreement between the model and experimental data.

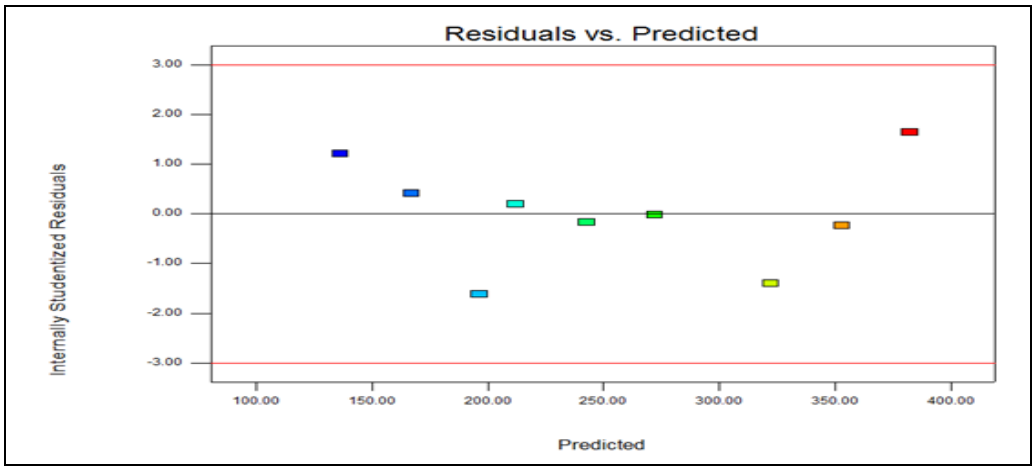

FIG. 3A: PREDICTED RESIDUALS VERSUS PREDICTED RESPONSE (PARTICLE SIZE) BY THE FINAL MODEL

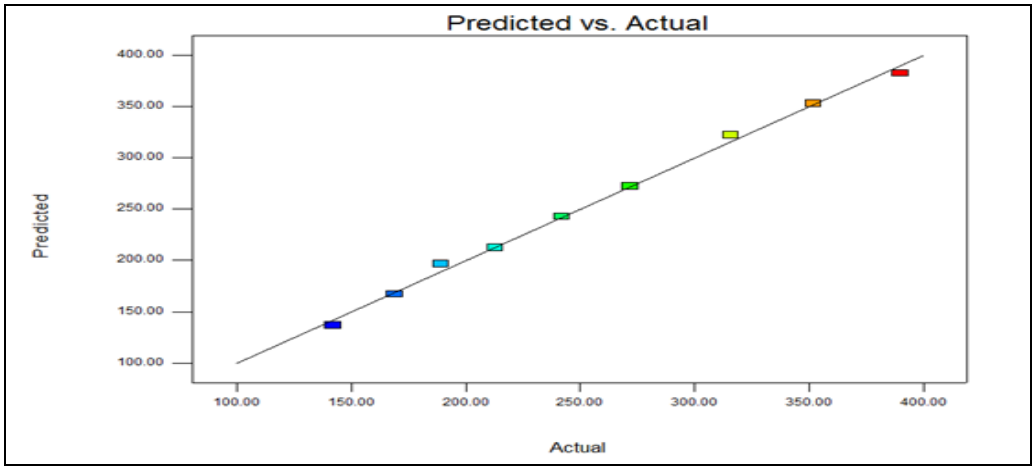

FIG. 3B: PREDICTED VERSUS ACTUAL VALUES OF PARTICLE SIZE BY THE FINAL MODEL

TABLE 4: ANOVA OF PRACTICAL YIELD AND PARTICLE SIZE

Variables	Source	Sum of squares	Df	Mean of squares	F ratio	Prob. > F	R2
Practical yield	Model	1317.678	4	329.4194	4328.139	< 0.0001	0.9998
	Residual	0.304444	4	0.076111			
	C.Total	1317.982	8				
Particle size	Model	57895.78	4	14473.94	302.943	< 0.0001	0.9967
	Residual	191.1111	4	47.77778			
	C.Total	58086.89	8				

Analysis Using S/N Ratio: In the Taguchi method, S/N ratio is a measure of quality characteristics and deviation from the desired value. The max-min values of reaction temperature and reaction time are the highest value. Therefore, it can understand that reaction temperature and reaction time are the significant factors that influence the practical yield **Table 5**.

TABLE 5: S/N RATIO TABLE FOR PRACTICAL YIELD AND PARTICLE SIZE

Run	Control factor	Practical yield (%) Mean S/N ratio (dB)				Particle size (nm) Mean S/N ratio (dB)			
		Level 1	Level 2	Level 3	Max-Min	Level 1	Level 2	Level 3	Max-Min
1	Reaction temperature	-36.37	-39.47	-38.69	3.1	-47.73	-47.55	-47.64	0.17
2	Reaction time	-37.88	-38.22	-38.43	0.54	-47.74	-47.51	-47.67	0.22
3	Stirring speed	-38.16	-38.17	-38.2	0.04	-50.91	-47.64	-44.37	6.53
4	Volume of solvent	-38.15	-38.19	-38.19	0.046	-46.53	-47.72	-48.68	2.14

Optimization and Confirmation Experiments: To verify the data, three batches of nanosponges with varied molar concentrations (1:2, 1:4, and 1:8) were prepared according to the predicted levels of A, B, C and D. The predicted and observed values are shown in **Table 6.** Obtained Y1 and Y2 values were in close agreement with the predicted values. The good agreement between the predicted and experimental results verified the validity of the model and the existence of an optimal point for the synthesis of nanosponges.

TABLE 6: RESULTS OF THE CONFIRMATION EXPERIMENT BY THE CONSTRAINTS APPLIES ON Y1 AND Y2

Independent variable	Nominal values	Predicted values		Observed values		
		Practical yield (Y1)	Particle size (Y2)	Batch	Practical yield (Y1)	Particle size (Y2)
Reaction temperature (A)	100	96.58	146.44	NS1	95.34±0.56	161± 2.4
Reaction time (B)	480			NS2	94.75±0.34	138± 3.2
Stirring speed (C)	3000			NS3	96.12 ± 0.73	155 ± 4.6
Volume of solvent (D)	100					

Characterization of Prepared Nanosponges: The particle size analysis of prepared nanosponges revealed that the average particle size measured by laser light scattering method is around 139-161 nm with low polydispersity index. A sufficiently high zeta potential values between -12 to -24 mV indicates that the complexes would be stable, and the tendency to agglomerate would be minuscule. A narrow PI means that the colloidal suspensions are homogenous in nature **Fig. 4, Table 7.**

TABLE 7: PARTICLE SIZE ANALYSIS OF CYCLODEXTRIN NANOSPONGE

Sample	Mean hydrodynamic diameter ± SD (nm)	Polydispersity Index	Zeta potential (mV)
NS1	161±2.4	0.45±0.005	-24.32±1.8
NS2	139±3.2	0.18±0.005	-12.18±1.3
NS3	155±4.5	0.645±0.005	-16.34±1.1

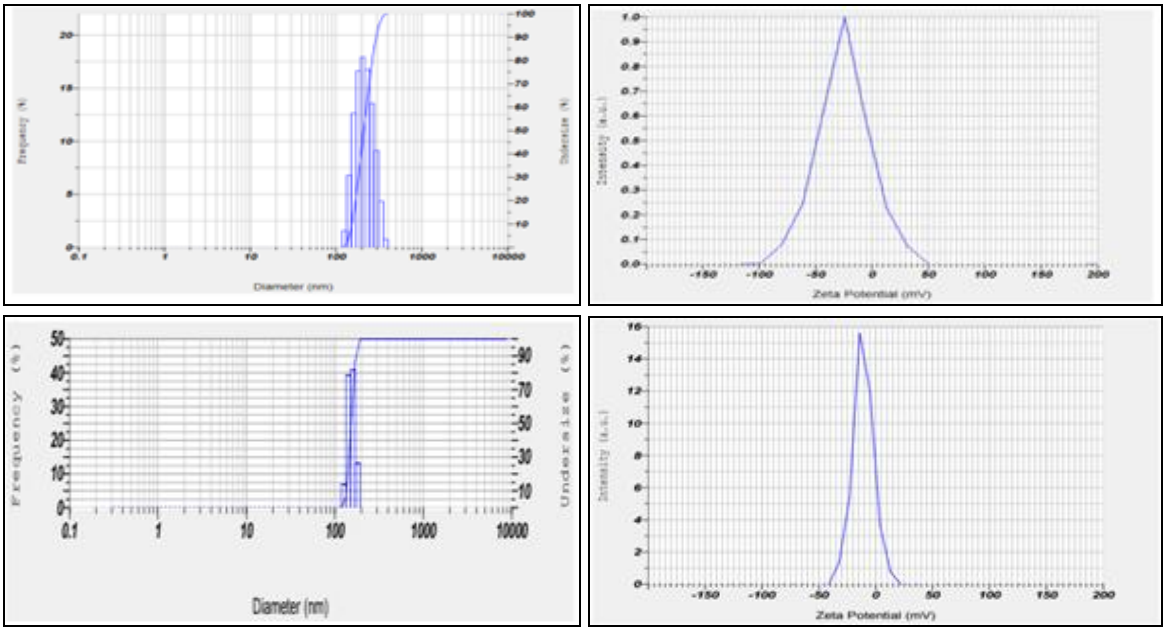

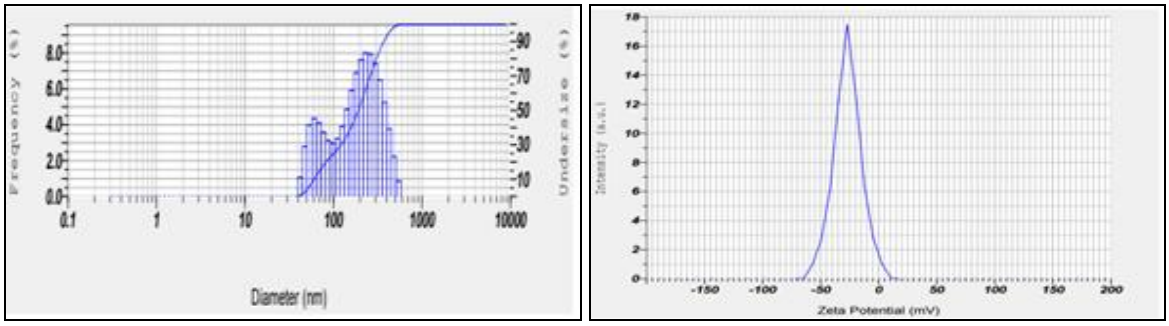

FIG. 4: PARTICLE SIZE AND ZETA POTENTIAL OF PREPARED NANOSPONGES

Fig. 5 shows a comparison of FTIR spectra of β-Cyclodextrin, NS1, NS2, and NS3. Plain nanosponge obtained under the optimal experimental showed a characteristic peak of carbonate bond at around 1720-1750 cm^{-1} which confirms the formation of cyclodextrin-based nanosponges. The peak at 1720-1750 cm^{-1} is missing in the FTIR spectrum of β-cyclodextrin, which is a starting material for nanosponge synthesis. In addition, the other characteristics peak of NS were found at 2918 cm-1 due to the C-H stretching vibration, 1418 cm^{-1} due to C-H bending vibration, and 1026 cm^{-1} due to C-O stretching vibration of primary alcohol.

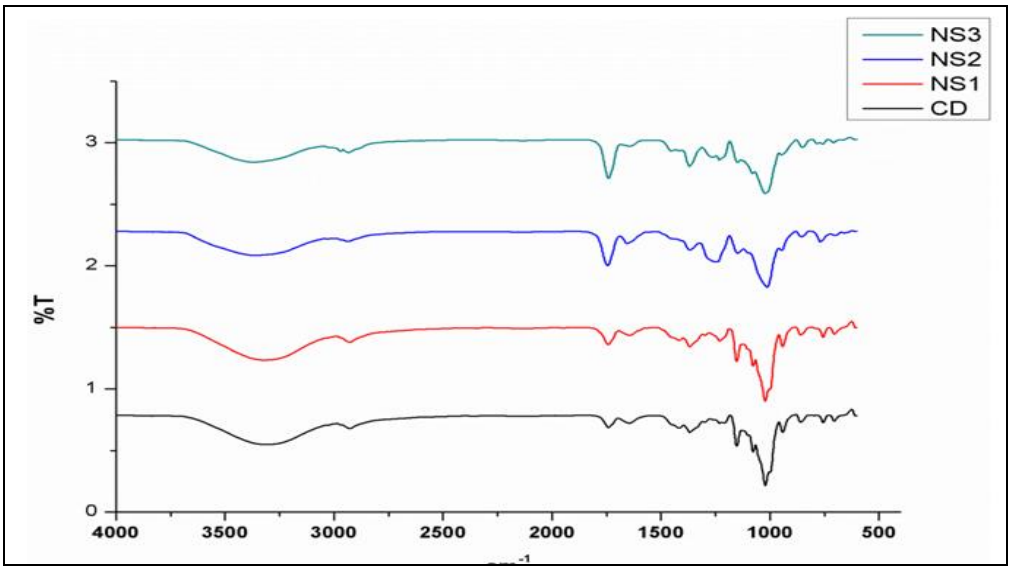

FIG. 5: FTIR SPECTRA OF B-CYCLODEXTRIN AND SYNTHESIZED NANOSPONGES (NS1-NS3)

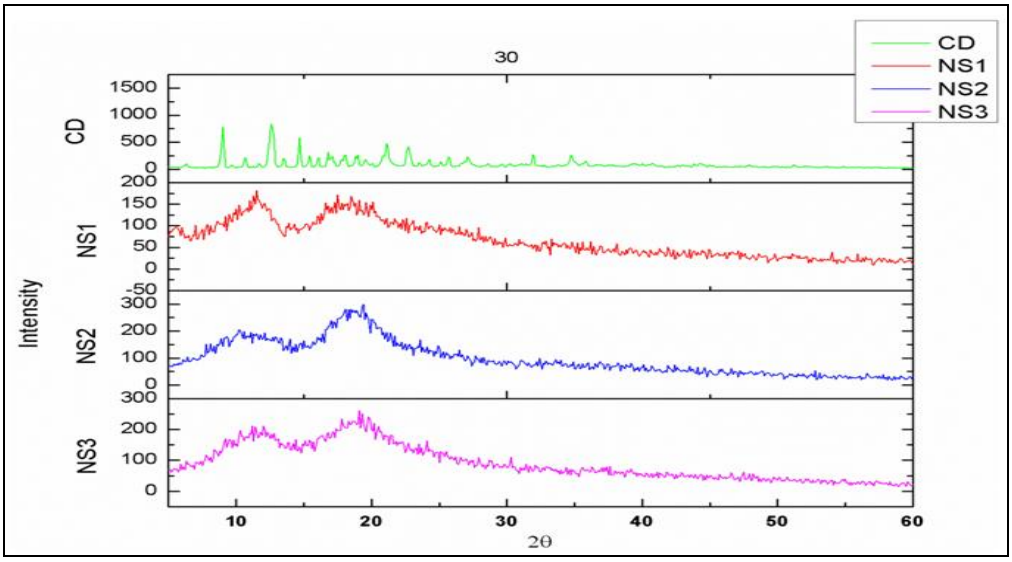

FIG. 6: XRPD PATTERN OF B-CYCLODEXTRIN AND SYNTHESIZED NANOSPONGES (NS1-NS3)

X-ray analysis was used to characterize the nano sponge solid structure. The plain β-Cyclodextrin (not cross-linked) showed a crystalline structure at XRPD as shown in **Fig. 6.** Whereas, XRPD pattern of nanosponges shows the crystallinity degree with a weak long-range order characterized by some broad reflections that appear as narrow peaks in the XRPD of β-Cyclodextrin. The short-range order being almost lost and represented only by some broad reflections indicating the formation of paracrystalline nanosponges. All the batches of nanosponges formed using different cross-linking ratios show very similar XRPD patterns.

Differential scanning analysis was performed to characterize the nanosponges. The DSC thermogram of β- cyclodextrin exhibited an endothermic peak at 290 °C correspondings to its melting transition point **Fig. 7.** The DSC analysis of nanosponges showed no peak before 350 °C, meaning that this material has high thermal stability. From the TEM images of **Fig. 3.11**, one can clearly observe that the obtained nanosponges exhibit nearly spherical shapes with homogeneous size distributions. TEM studies showed that the regular spherical shape and sizes of nanosponges **Fig. 8.**

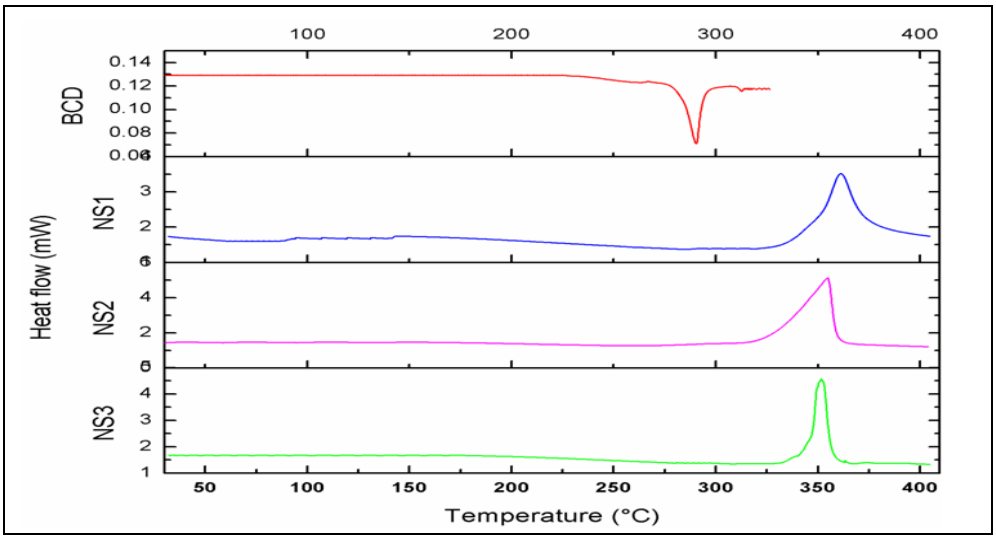

FIG. 7: DSC THERMOGRAM OF B-CYCLODEXTRIN AND SYNTHESIZED NANOSPONGES (NS1-NS3)

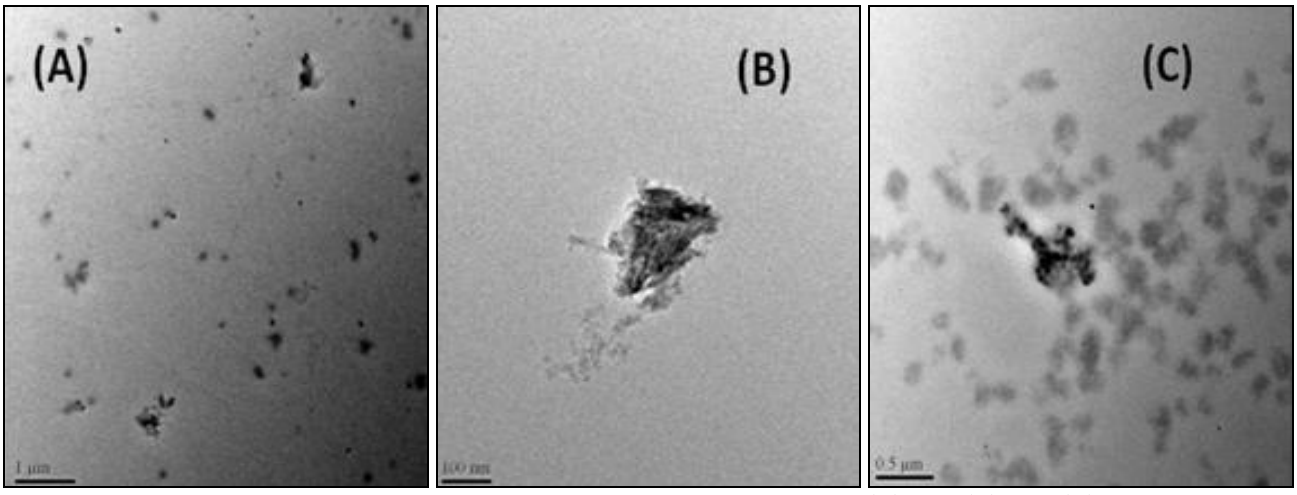

FIG. 8: TEM IMAGES OF SYNTHESIZED NANOSPONGES (A) NS1 (B) NS2 (C) NS3

Evaluation of Drug Loaded Nanosponges: Among the three types of nanosponges, the loading efficiency was found to be higher in IBNS2 (1:4 β-Cyclodextrin: Carbonyldiimidazole) as much as 48% w/w. Considering high drug loading capacity, IBNS2 was used for further studies.

TABLE 8: PERCENT DRUG LOADING IN NANOSPONGES

S. no.	Name of the formulation	Drug loading (%)
1	IBNS1	23 ± 0.92
2	IBNS2	48 ± 0.63
3	IBNS3	29± 0.88

(all determinations were performed in triplicate and values were expressed as mean ± s.d., n=3)

In-vitro Release of Ibrutinib from Nanosponge Formulations: From *in-vitro* release studies, it was found that the nano sponge-loaded formulations showed a significant improvement in the rate of release as compared with the pure drug. The drug release from the nanosponge formulations is highly significant as compared to free drug suspension ($P < 0.05$). More than 90 % of the drug was released from nanosponge formulations compared to only around 21% from free drug suspension after 24 h of study (**Fig. 9.**

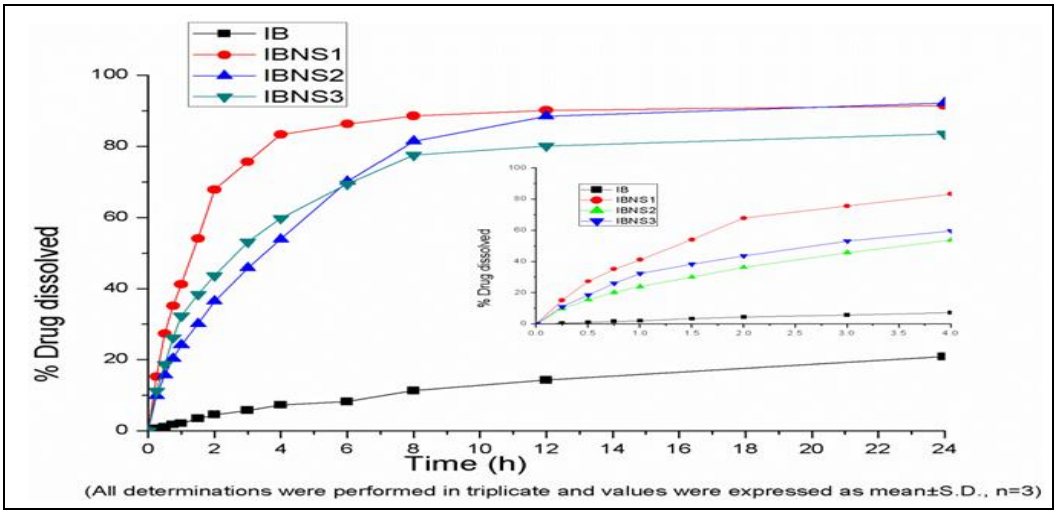

FIG. 9: DISSOLUTION PROFILE OF PURE IBRUTINIB AND IBRUTINIB LOADED NANOSPONGE FORMULATIONS

Various mathematical models were applied to evaluate the mechanism of drug release from nanoformulation. Drug release data for the formulation (IBNS2) was fitted into various kinetic equations to find out the order and mechanism of drug release. The correlation coefficient showed that the release profile followed the Korsemeyerpeppas (R2= 0.7224), Also from the Korsemeyerpeppas model, the release exponent, n was found to be 0.231 (0.43 > n) and followed anomalous behaviour and release mechanism was indicative of diffusion.

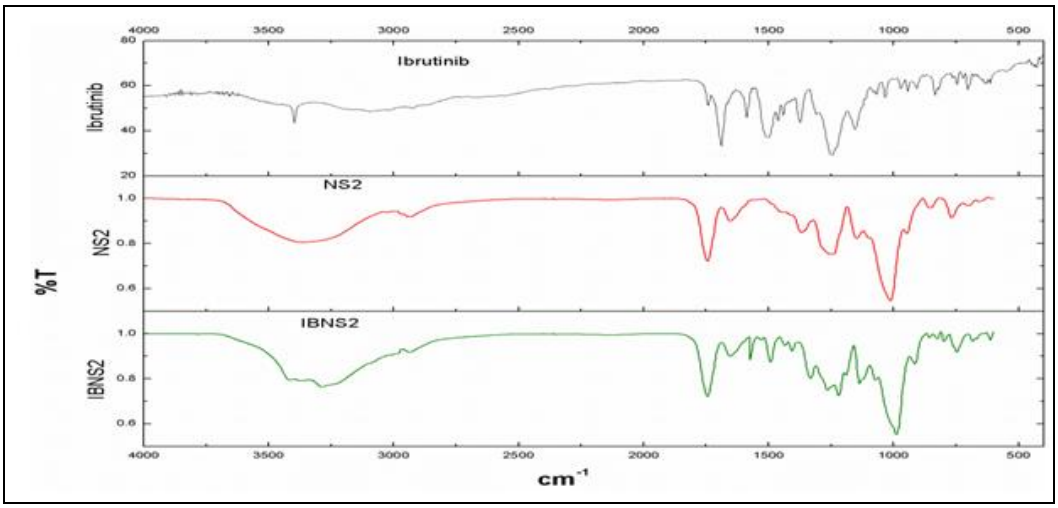

FIG. 10: FTIR SPECTRA OF FREE IBRUTINIB, PLAIN NANOSPONGES (NS2) AND IBRUTINIB LOADED NANOSPONGE COMPLEXES (IBNS2)

Characterization of Plain (NS2) and drug Loaded Nanosponge Complexes (IBNS2): Fig. 10 shows a comparison of FTIR spectra of Ibrutinib, NS2, and IBNS2 complex. Plain nanosponge showed a characteristic peak of carbonate bond at around 1740-1750 cm^{-1} which confirms the formation of cyclodextrin-based nanosponges. Other characteristics peaks of nanosponges were found at 2918 cm^{-1} due to the C-H stretching vibration, 1418 cm^{-1} due to C-H bending vibration, and 1026 cm^{-1} due to C-O stretching vibration of primary alcohol. The

Comparison of FTIR spectra of ibrutinib and ibrutinib complex (IBNS2) showed that there is a major change in the fingerprint region, *i.e.,* 900 to 1,400 $cm^{-1,}$ as the main characteristic peaks of ibrutinib were broadened or shifted in the formulations suggesting definite interactions between ibrutinib and nanosponges. The DSC thermogram of free drug shows a sharp melting point at approximately 159 °C indicating the crystalline nature of the drug. The DSC thermogram of plain nanosponges (NS2) showed exothermic peaks at around 350 °C. Ibrutinib nanosponge complex (IBNS2) also exhibited a broad exothermic peak at around 350 °C. The complete disappearance of ibrutinib endothermic peak was observed for the formulation **Fig. 11.**

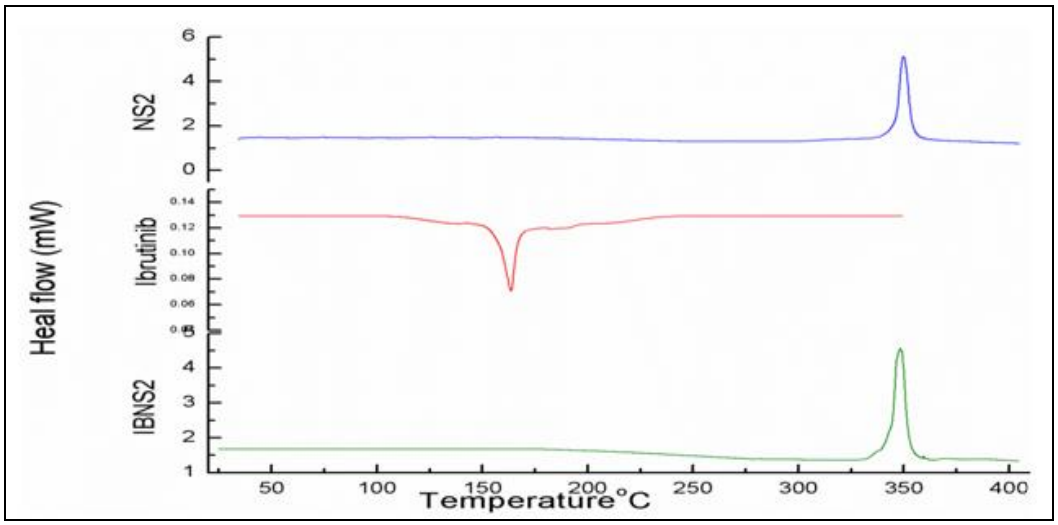

FIG. 11: DSC THERMOGRAMS OF PLAIN NANOSPONGES (NS2), FREE IBRUTINIBANDIBRUTINIB LOADED NANOSPONGE COMPLEXES (IBNS2)

The x-ray diffractograms of plain ibrutinib exhibited sharp, intense peaks at 2θ values of 5.6 °C, 13.5 °C, 16.5 °C, 19.2 °C, 21.2 °C, and 21.7 °C confirming the drug's crystal form as shown in **Fig. 12.** However, there was no characteristics peaks of pure ibrutinib were observed in NS complexes. The absence of such crystalline peaks of ibrutinibin nano sponge complex clearly indicates that the drug is encapsulated in nanosponges.

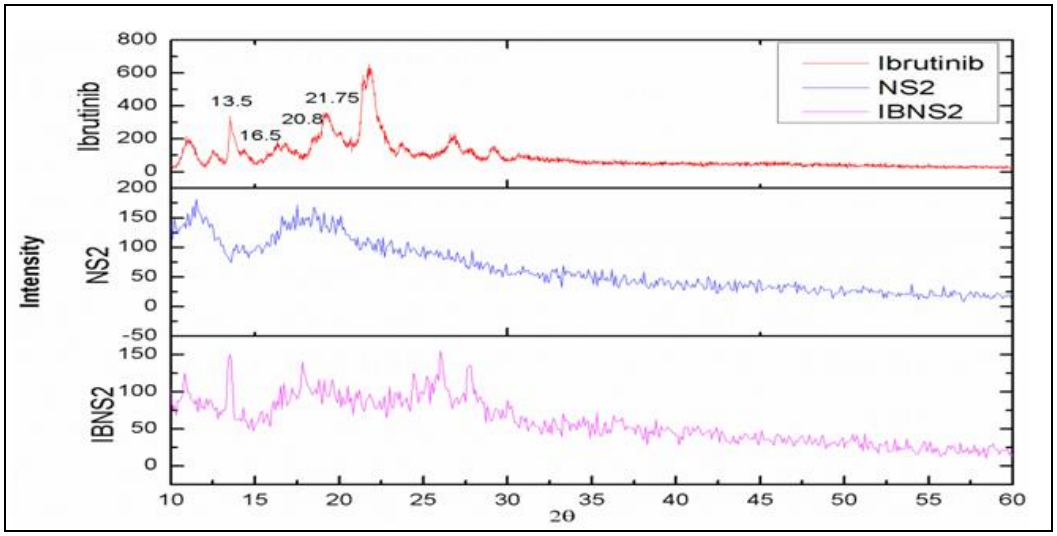

FIG. 12: XRPD PATTERN OF IBRUTINIB, PLAIN NANOSPONGES (NS2) AND IBRUTINIB LOADED NANOSPONGE COMPLEXES (IBNS)

Morphology and Sizes of The Ibrutinib Loaded Nanosponges (IBNS2): The particle size analysis of plain nanosponges and ibrutinib loaded nanosponges revealed that the average particle size measured by laser light scattering method is around 138-171 nm with low polydispersity index. A

narrow polydispersity index means that the colloidal particles are homogenous in nature. A sufficiently high zeta potential indicates that the complexes would be stable, and the tendency to agglomerate would be miniscule. The entire formulations prepared were found to be fine and free-flowing powders. The particle size distribution and zeta potential values are shown in **Fig. 13.** Transmission electron microscopy (TEM) studies showed that the regular spherical shape and size of plain nanosponges are unaffected even after drug encapsulation. The particle size of the complexes as observed under TEM was consistent with the data obtained through dynamic light scattering **Fig. 13.**

TABLE 9: PARTICLE SIZE, POLYDISPERSITY INDEX AND ZETA POTENTIAL OF PLAIN NANOSPONGES AND DRUG-LOADED NANOSPONGE FORMULATION

Sample	Mean hydrodynamic diameter ± SD (nm)	Polydispersity Index	Zeta potential (mV)
NS2	138.2 ± 3.2	0.18 ± 0.005	-12.18 ± 1.2
IBNS2	171.4 ± 2.3	0.21 ± 0.005	-21.6 ± 2.1

(All determinations were performed in triplicate and values were expressed as mean±S.D., n=3)

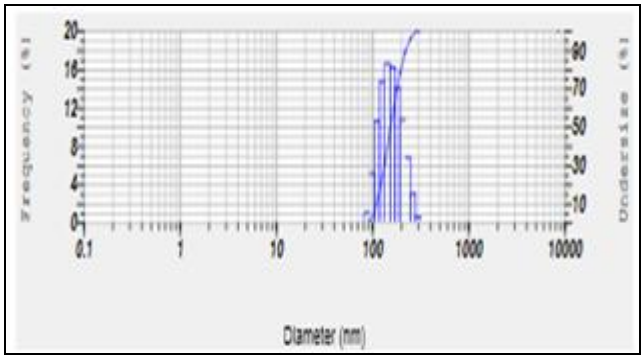

PARTICLE SIZE DISTRIBUTION OF PLAIN NANOSPONGES (NS2)

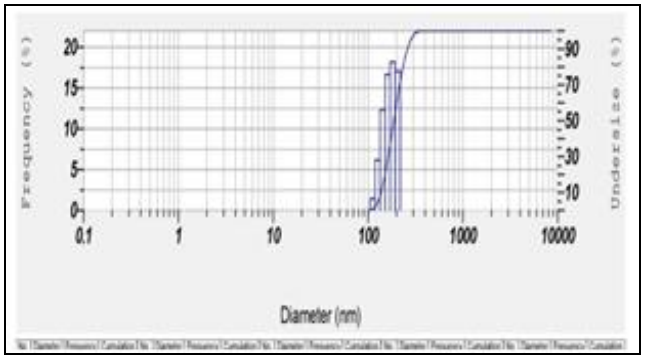

PARTICLE SIZE DISTRIBUTION OF IBRUTINIB LOADED NANOSPONGES (IBNS2)

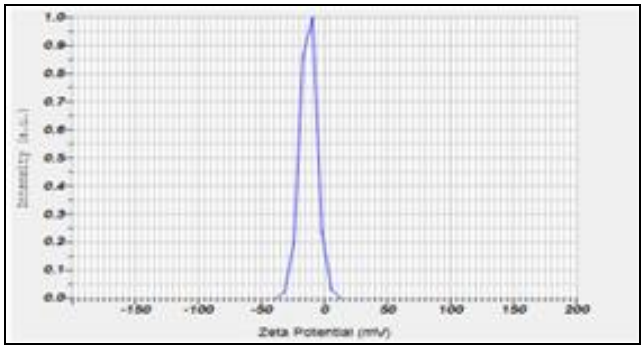

ZETA POTENTIAL OF PLAIN NANOSPONGES (NS1)

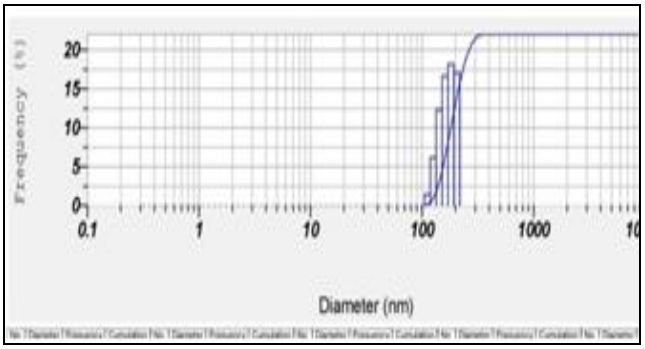

ZETA POTENTIAL OF IBRUTINIB LOADED NANOSPONGES (IBNS2)

FIG. 13: PARTICLE SIZE AND ZETA POTENTIAL OF NS2 AND IBNS2

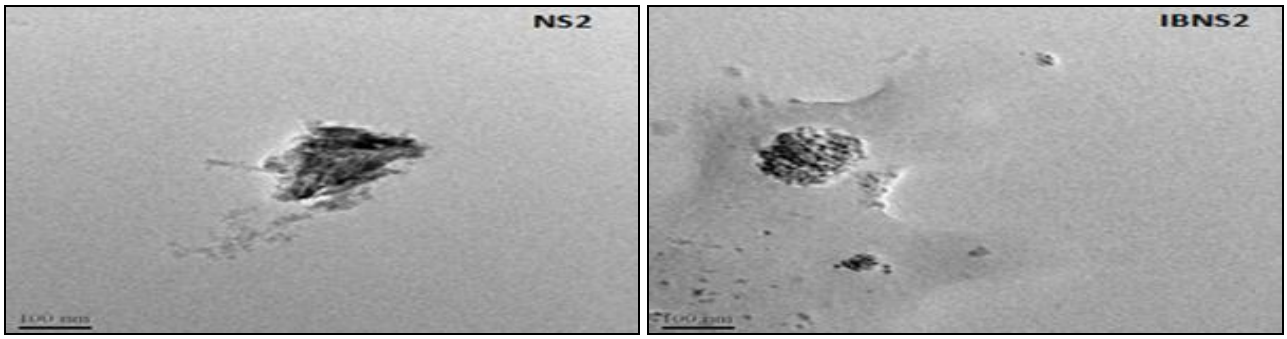

FIG. 14: A. TEM IMAGE OF PLAIN NANOSPONGES (NS2) B. IBRUTINIB LOADED NANOSPONGE COMPLEXES

CONCLUSION: The present study demonstrated the preparation of ibrutinib-loaded nanosponges by freeze-drying technique. FTIR, DSC, and XRD studies confirmed the formation of the inclusion

complex of ibrutinib with nanosponges. The dissolution of the ibrutinib nanosponges was significantly higher compared with the pure drug due to the reduction of drug particle size, the formation of a high-energy amorphous state and the intermolecular hydrogen bonding. The release kinetics may be prolonged or accelerated according to the type of nanosponges. Hence, it can be concluded that cyclodextrin-based nanosponges of ibrutinib offer a potential drug delivery system for oral and topical delivery. Overall, this research demonstrated the use of cyclodextrin nanosponges as an effective carrier of anticancer drug ibrutinib to improve its physicochemical properties, oral bioavailability, and therapeutic efficacy.

ACKNOWLEDGEMENT: Nil

CONFLICTS OF INTEREST: Nil

REFERENCES:

1. Swaminathan S, Pastero L, Serpe L, Trotta F, Vavia P, Aquilano D, Trotta M, Zara G and Cavalli R: Cyclodextrin-based nanosponges encapsulating camptothecin: Physicochemical characterization, stability and cytotoxicity. Eur J Pharm Biopharm 2010; 74: 193-01.
2. Kishore R, Vinaydas A, Kavitha JR and Swathi V: Cyclodextrins: nanocarriers for novel drug delivery. Int J Pharm 2012; 2(1): 109-16.
3. Amin A and Ranjana HA: Bruton's tyrosine kinase inhibitors and their clinical potential in the treatment of B-cell malignancies: focus on ibrutinib. The rAdvHematol 2014; 5(4): 121-33.
4. Haura EB and Rix U: Deploying ibrutinib to lung cancer: another step in the quest towards drug repurposing. J Natl Cancer Inst 2014; 106(9): 250.
5. Allahyari S, Trotta F, Valizadeh H, Jelvehgari M and Zakeri-Milani P: Cyclodextrin-based nanosponges as promising carriers for active agents. Expert Opin Drug Deli 2019; 16(5): 467-79.
6. Taguchi G: Tables of orthogonal arrays and linear graphs maruzen. Tokyo Japan 1962.
7. Swaminatha S, Vavia PR and Trotta F: Structural evidence of differential forms of nanosponges of beta-cyclodextrin and its effect on solubilization of a model drug. J Incl Phenom Macrocycl Chem 2013; 76: 201-11.
8. Kacker RN, Lagergren ES and Filliben JJ: Taguchi's orthogonal arrays are classical designs of experiments. J Res Natl Inst Stand Technol 1991; 96(5): 577-91.
9. Bindiya P, Om B, Kuldeep R, Riddhi P and Varsha A. An assessment on preparations, characterization, and poles apart appliances of nanosponge. International Journal of Pharm Tech Research 2010; 6(6): 1898-07.
10. Nagarjun Rangaraj, Sravanthi Reddy Pailla, Paramesh Chowta and Sunitha Sampathi: Fabrication of ibrutinib nanosuspension by quality by design approach: intended for enhanced oral bioavailability and diminished fast fed variability. AAPS Pharm Sci Tech 2019; 20: 326.
11. Qiu Q, LuM, Li C, Luo X, Liu X and Hu L: Novel self-assembled ibrutinib-phospholipid complex for potently peroral delivery of poorly soluble drugs with pH-dependent solubility. AAPS Pharm Sci Tech 2018; 19(8): 3571-83.
12. Shakeel F: Solubility and thermodynamic function of a new anticancer drug ibrutinib in 2-(2- ethoxyethoxy) ethanol + water mixtures at different temperatures. J Chem Thermodyn 2015; 89: 151-55.
13. Costa P and Lobo JMS: Modeling and comparison of dissolution profiles. Eur J Pharm Sci 2001; 15: 123-33

How to cite this article:
Surender G and Ramesh B: Formulation and characterization of ibrutinib loaded cyclodextrin nanosponges. Int J Pharm Sci & Res 2022; 13(2): 930-41. doi: 10.13040/IJPSR.0975-8232.13(2).930-41.